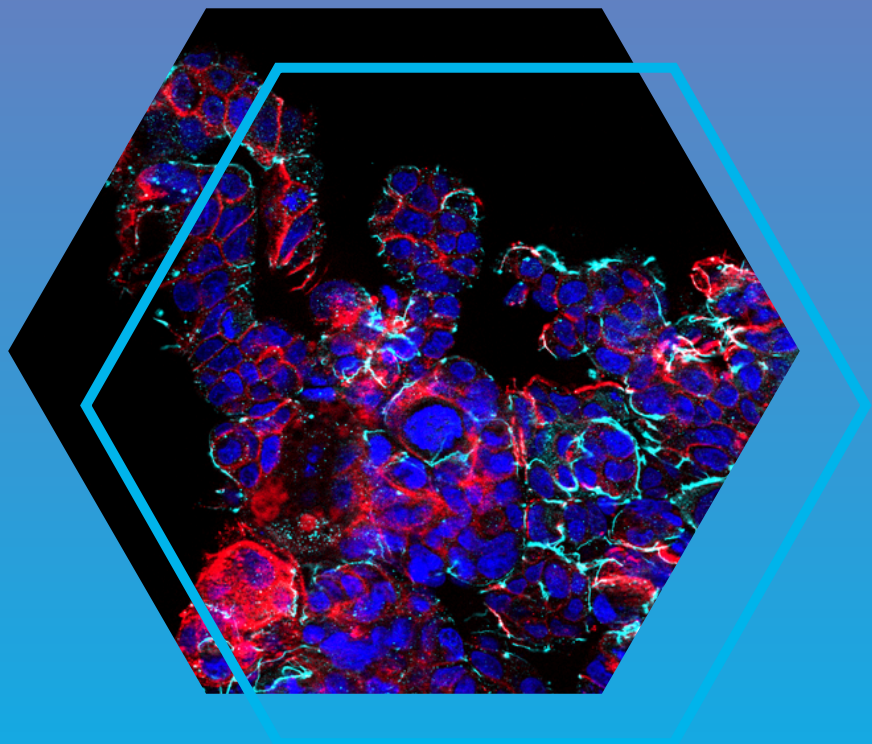




Application
Note

Modeling fungal infection in an intestine-on-chip

Investigating effectiveness of the
antifungal drug caspofungin on *Candida
albicans* growth and pathogenicity



Author:
Tim Kaden

Release date:
09/01/2025

Important - please read

It is important to note that due to donor variability, monocyte-derived macrophages (MDMs) from different donors may exhibit variations in their response to different drug compounds. Consequently, this variability among different biological replicates should be considered in the interpretation of experimental results.

Abstract

The intestine is a major reservoir for many fungal species within the human body. The fungus *Candida albicans* is usually a non-harmful commensal of the gastrointestinal tract, but is also among the most relevant species causing life-threatening invasive candidiasis. Invasive candidiasis usually originates from the intestine upon predisposing conditions such as immunosuppression, chemotherapy or antibiotic treatment, chronic inflammation, or invasive surgical interventions. Under these circumstances, *C. albicans* can form invasive microcolonies, breach the intestinal epithelial barrier, and disseminate into the bloodstream, leading to infection of vital organs.

Fungal-host interactions during candidiasis are normally studied using 2D *in vitro* or animal models. Human cell-based microphysiological models, so-called organ-on-chip models, present an alternative that may better mimic *in vivo*-like infection processes and antifungal drug efficacy. Such systems offer a higher degree of complexity, integration of biomechanical stimulation, and the possibility of intravenous drug application. Therefore, a 3D intestine-on-chip model was leveraged to investigate fungal-host interactions upon infection with *C. albicans* and to investigate antifungal caspofungin treatment under clinically relevant conditions. By combining microbiological and image-based analyses, it was possible to quantify biological host alterations and to obtain novel in-depth insights into fungal microcolony morphology.

We were able to demonstrate that *C. albicans* microcolonies induce epithelial tissue damage and inflammation. Caspofungin treatment effectively reduced the fungal biomass and induced alterations in microcolony morphometrics, resulting in decreased fungal pathogenicity and reduced host injury. In comparison, caspofungin showed limited effects on an echinocandin-resistant clinical isolate of *C. albicans*.

By bridging the gap between conventional *in vitro* models and *in vivo* studies, the intestine-on-chip platform is a promising tool to evaluate fungal infections and underlying alterations in host-microbiota interactions, and to improve antifungal drug development strategies.

Highlights

- The near-physiological intestine-on-chip candidiasis model recapitulates relevant pathogen-host interactions leading to systemic candidiasis
- Vascular perfusion of antifungal caspofungin at clinically relevant concentrations prevents intestinal *C. albicans* infection for a wild-type strain but not for an echinocandin-resistant strain
- Caspofungin affects the morphology of microcolonies and reduces *C. albicans* invasiveness, fungal burden, disruption of the intestinal barrier, and host immune response
- Development of algorithms for automated analysis of microscopy images for quantification of microbiological readouts

Introduction

C. albicans is a common commensal of the human mycobiota, residing in the gastrointestinal tract of most individuals (Gouba & Drancourt, 2015). However, under predisposing conditions such as immunosuppression, chemotherapy, antibiotic use, or invasive surgeries (Koh et al., 2008; Pfaller et al., 2005; Wisplinghoff et al., 2004), the fungus can transition to a pathogenic state, forming invasive hypha filaments to invade the intestinal tissue and translocate into the bloodstream. This can lead to invasive candidiasis and life-threatening infections of other vital organs (Miranda et al., 2009; Zhai et al., 2020). First-line treatments, such as the echinocandin caspofungin, are often ineffective due to fungal resistance and limitations in biophysical drug properties (Fisher et al., 2022). This necessitates new therapeutic approaches and a more advanced understanding of antifungal effects on pathogen-host interactions.

Traditional *in vitro* models, often based on intestinal epithelial cell monolayers, and animal models, primarily mice, have provided seminal insights (Allert et al., 2018; Alonso-Roman et al., 2022; Graf et al., 2019; Ruiz Mendoza et al., 2022) but fail to fully mimic the processes during human infection. 2D *in vitro* systems often lack *in vivo*-like tissue morphology, immune cell presence, and biomechanical stimulation, while interspecies differences in animal models limit the extrapolation of results to humans. Moreover, mouse strains can be resistant to *C. albicans* colonization (Miranda et al., 2009; Naglik et al., 2008), requiring external manipulation with antibiotics (Koh et al., 2008; Mellado et al., 2000), immunosuppression (Kobayashi-Sakamoto et al., 2018), or removal of the microbiome (Balish et al., 2005). These challenges highlight the need for human cell-based models that recapitulate host-pathogen-drug interactions in a human physiological manner.

To address these limitations, a microphysiological intestine-on-chip model (Maurer et al., 2019) was used to explore *C. albicans* infection and intravascular antifungal treatment at human relevant concentrations. The combination of organ-on-chip technology, microbiological analyses, and advanced image-based investigation allowed to assess insights into fungal pathogenicity mechanisms, host responses, and influence of antifungal treatment on host-pathogen interactions.

Materials and Methods

The materials and methods outlined in this application note closely follow those outlined in Kaden, Alonso-Roman, Akbarimoghaddam et al., 2024. Any modifications or adaptations made to the protocol are clearly specified.

Peristaltic pump

(can be purchased in line with the DynamicOrgan System)

DynamicOrgan Developers Kit

Including:

- / Biochips (BC002)
- / 2-Stop Tubing
- / Connectors (Adapter)
- / Reservoirs



Cells

- Caco-2
- Human umbilical vein endothelial cells (HUVECs)
- Monocyte-derived macrophages (MDMs)

Fungal strains

- Wild-type strain: *C. albicans* SC5314
- Echinocandin-resistant strain: *C. albicans* 110.12

Media and reagents

- Endothelial cell growth medium (ECGM MV) + supplements
- Vascular perfusion medium 2 (VPM2): ECGGM MV + autologous serum + supplements
- Gut seeding medium (GSM): DMEM + 20% FBS + supplements
- Gut maintenance medium (GMM): DMEM + 10% FBS + supplements
- Gut infection medium: DMEM
- Caspofungin diacetate ($\geq 97\%$, CAS number: 179463-17-3)

Results

1. 1. The intestine-on-chip model for infection modeling and antifungal drug evaluation

BC002, a Dynamic42 biochip, containing an integrated polyethylene-terephthalate (PET) membrane with randomly distributed pores (median density: $1 \times 10^5/\text{cm}^2$) of 8 μm in diameter, was used as a platform to build the intestinal model. Human umbilical vein endothelial cells (HUVECs) were seeded in the bottom channel (Figure 1) and were statically cultured upside-down for 2 days to facilitate attachment to the membrane. After reaching confluency, monocyte-derived macrophages (MDMs) were seeded on top of the HUVECs. Intestinal Caco-2 cells were seeded in the top channel. Up to this point, the biochips were maintained under static conditions. One day after seeding the Caco-2 cells, bidirectional perfusion of the top and bottom channels was initiated using a peristaltic pump. The appropriate medium was circulated from a microfluidic reservoir through both channels in a circular-loop system, with medium exchange after 3 days. Subsequently, circular perfusion in the top channel was switched to linear perfusion to infect the model with *C. albicans*. The bottom vascular channel remained under circular perfusion. *C. albicans* cells were pipetted into the microfluidic reservoir of the top channel, and the models were infected for 10 minutes under perfusion. Caspofungin was applied in vascular perfusion medium 2 (VPM2) within the vascular channel for up to 24 hours.

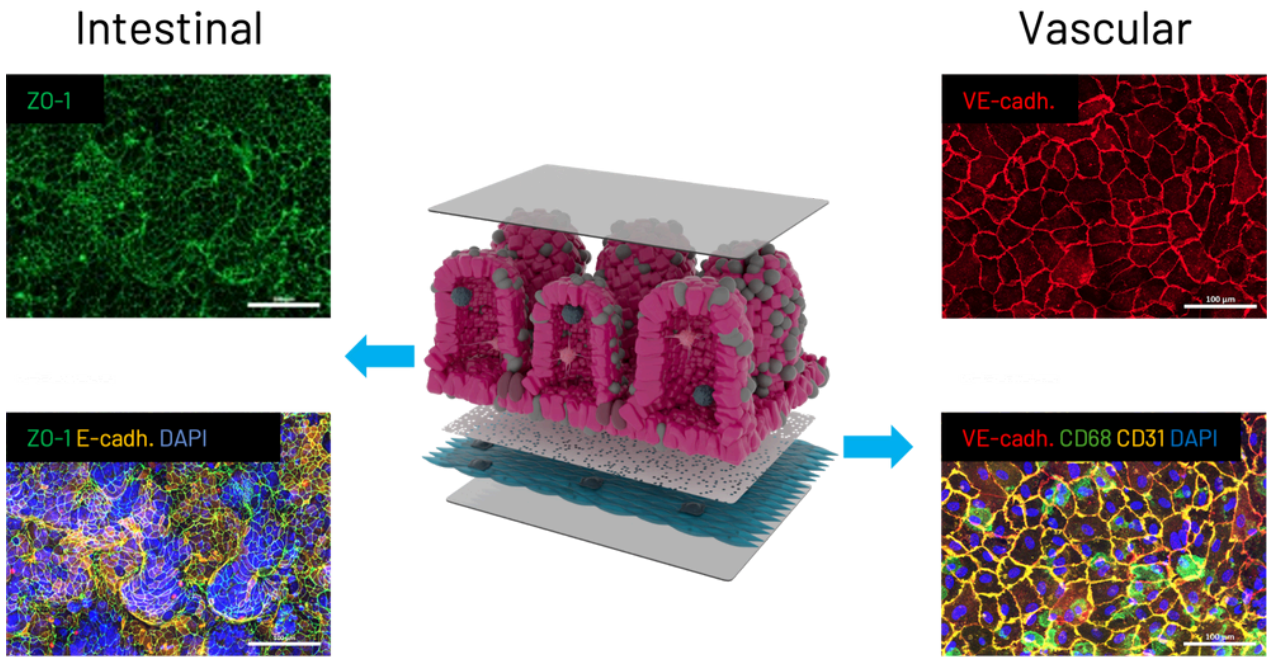


Figure 1: Immunofluorescence staining of: left panel: intestinal cell layer by zonula occludens-1 (ZO-1, green), epithelial cadherin (E-cadh., orange), and nuclei (DAPI, blue); right panel: vascular cell layer by vascular endothelial cadherin (VE-cadh., red), cluster of differentiation 68 (CD68, green), cluster of differentiation 31 (CD31, orange), and nuclei (DAPI, blue); mid-panel: 3D view of the intestine-on-chip model including intestinal epithelial cells (purple) and the vascular cell layer comprising endothelial cells (turquoise) and macrophages (dark blue). Scale bars = 100 μ m.

2. *C. albicans* infection in the intestine-on-chip model

C. albicans was inoculated under dynamic perfusion, resulting in colonization of the tissue. At 12 hours post infection (hpi), *C. albicans* formed microcolonies on the intestinal epithelium, characterized by filamenting hyphae growing in multiple directions (Figure 2A upper right image). Microcolonies were macroscopically visible after 24 hpi (Figure 2A middle image), spreading across the tissue and further invading the vascular compartment through the porous membrane (Figure 2A lower right image). These microcolonies caused a reduction in E-cadherin staining (Figure 2B), indicating disrupted cellular junctions and loss of barrier integrity. The endothelial tissue showed similar damage with disrupted CD31 signals (Figure 2B). The decrease in DAPI signals additionally indicated elevated cell death nearby the microcolonies (Figure 2C). By quantifying the area fraction of E-cadherin and CD31 it was found that these markers were drastically reduced in close proximity to *C. albicans* microcolonies (Figure 2D).

Moreover, intestinal epithelial barrier permeability was increased compared to non-infected models (Figure 2E). Cytokine release was further measured to investigate immune cell activation. Upon fungal invasion, pro-inflammatory cytokines (IL-1 β , IL-6, IL-8) and the anti-inflammatory cytokine IL-10 were elevated (Figure 2F), suggesting immune activation, although the cytokine levels did not reach significance due to donor variation. Cytokine levels in the intestinal were mostly undetectable due to dilution by the linear perfusion (Figure 3,4).

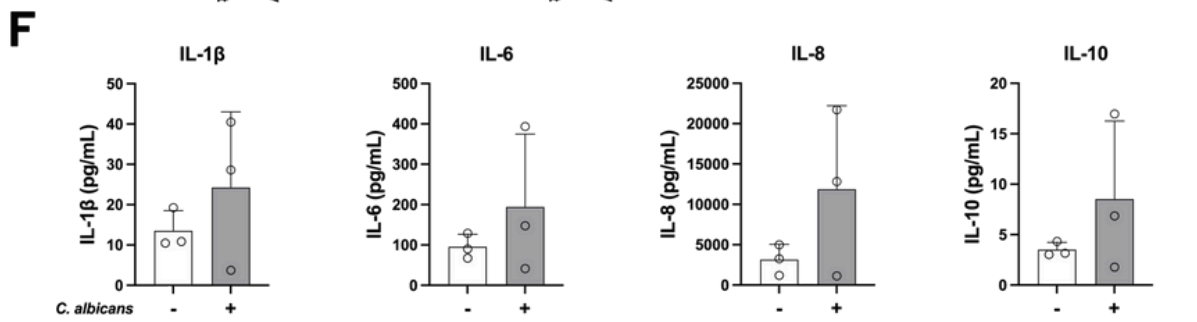
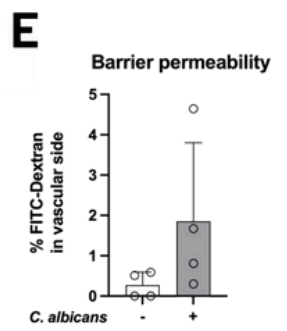
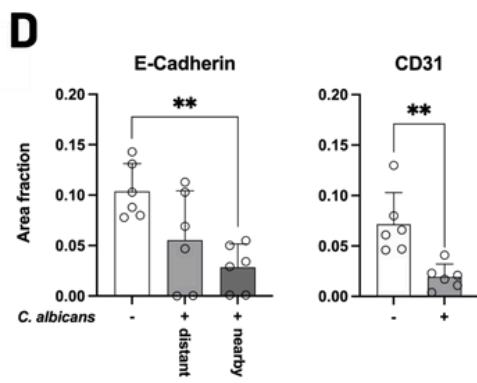
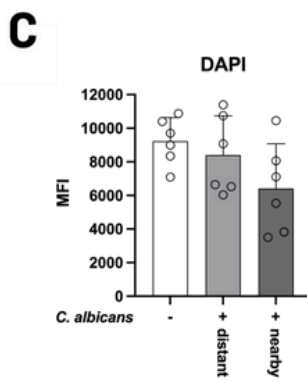
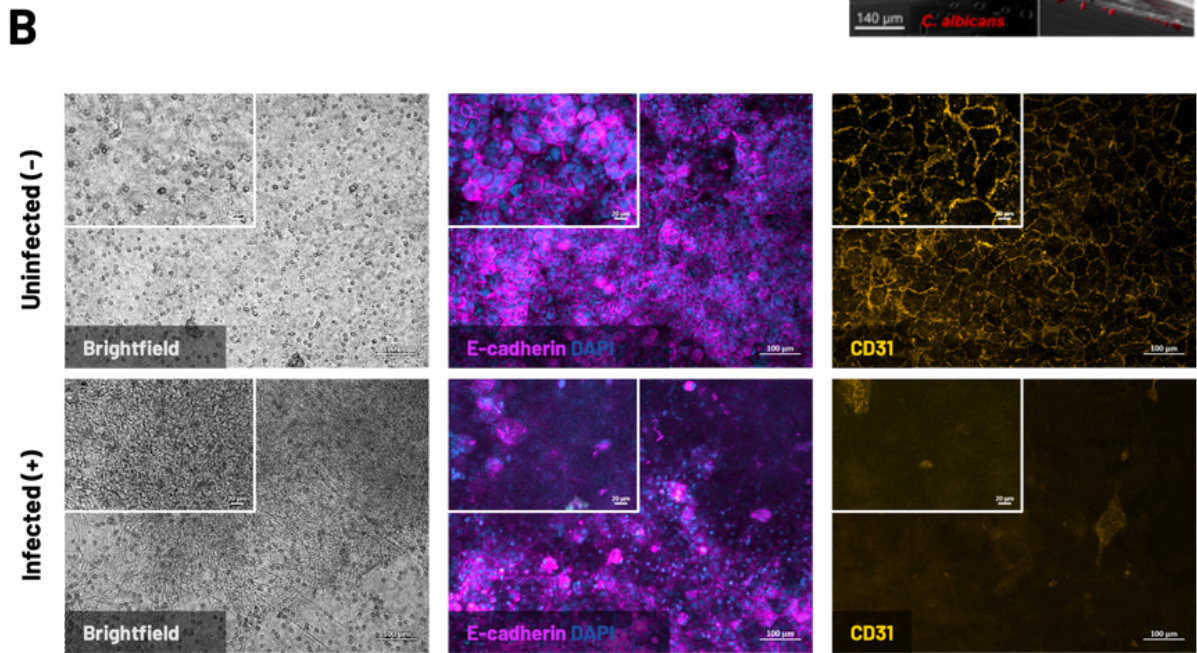
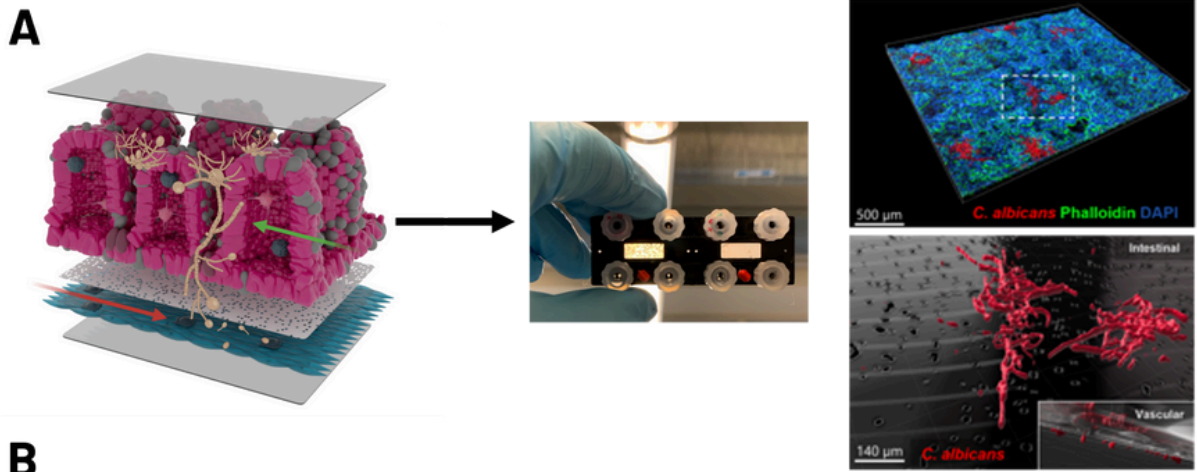


Figure 2: Infection of the intestine-on-chip model with *C. albicans* SC5314. A) Schematic image of the intestine-on-chip model composition (left image). Illustration of a biochip infected with *C. albicans* for 24 h (middle image). Microcolonies are visible within the intestinal compartment in the left chip cavity. The right images depict representative 3D reconstructions of the intestinal epithelial cell layer 12 hpi with *C. albicans* SC5314 (upper right image; *C. albicans*: red, F-Actin: green, nuclei: blue). Scale bar = 500 μm . Enlarged sections (bottom right image; *C. albicans*: red) of intestinal and vascular layers reveal *C. albicans* translocation through the membrane pores to the vascular side. Scale bar = 140 μm . Surface reconstruction was done using IMARIS 10.0.1 (Bitplane, Switzerland). B) Immunofluorescence and brightfield images of intestinal cell layers from intestinal models 24 hpi stained for the apical junction complex E-cadherin (purple) and nuclei (DAPI, blue) and vascular cell layers stained for CD31 (orange). Scale bars = 100 μm . Representative images from $n = 3$ biological replicates. C) Measurement of mean fluorescence intensity (MFI) of DAPI signals in the intestinal cell layer of either uninfected (-) or infected (+) models, with nearby or distant area analysis. D) Quantification of the area fraction of E-cadherin (intestinal) and CD31 (vascular) for uninfected (-) models and for regions nearby and distant from microcolonies in infected (+) models. Bars represent mean \pm SD of 3 independent experiments ($n = 3$) with 3 independent MDM donors. $**p \leq 0.01$ (Unpaired two-tailed t-test). Bars represent mean \pm SD of 3 independent experiments ($n = 3$) with 3 independent MDM donors. E) Permeability of the intestine-on-chip for FITC-Dextran (3–5 kDa) uninfected (-) or infected (+) with *C. albicans* SC5314, at 24 hpi. Permeability is quantified as the % of FITC-Dextran in the vascular compartment compared to the total FITC-Dextran added into the epithelial compartment. Bars indicate the mean \pm SD of 4 independent experiments ($n = 4$). F) Measurement of cytokines (IL-1 β , IL-6, IL-8, IL-10) collected from vascular medium supernatants of uninfected (-) or infected (+) models after 24 hpi. Bars represent mean \pm SD of 3 independent experiments ($n = 3$) with 3 independent MDM donors.

3. Candidiasis-on-chip model as a tool for assessing the antifungal activity of caspofungin

The antifungal efficacy of caspofungin, an echinocandin-class drug, was further investigated in the candidiasis-on-chip model. Caspofungin was perfused at clinically relevant concentrations (0.25 $\mu\text{g}/\text{mL}$, 1 $\mu\text{g}/\text{mL}$, and 4 $\mu\text{g}/\text{mL}$) (Stone et al., 2002) through the bottom vascular channel of the chip (Figure 3A). It was demonstrated that caspofungin was effective in reducing *C. albicans* microcolonies 24 hpi (Figure 3B). Moreover, caspofungin reduced intestinal fungal burden (Figure 3C), fungal invasion (Figure 3D), and dissemination (Figure 3E) in a concentration-dependent manner. By using the highest concentration of 4 $\mu\text{g}/\text{mL}$, caspofungin nearly completely inhibited fungal translocation to the vascular compartment (Figure 3E). The reduction of fungal microcolonies and overall fungal burden was also associated with a decrease in cytokine release. Caspofungin already reduced levels of IL-1 β , TNF- α , IL-6, IL-8, and IL-10 at a concentration of 0.25 $\mu\text{g}/\text{mL}$ in infected models (Figure 3F). The highest concentration of 4 $\mu\text{g}/\text{mL}$ caspofungin significantly decreased IL-1 β and IL-8 levels compared to uninfected models. Measurements in uninfected models treated with 4 $\mu\text{g}/\text{mL}$ caspofungin excluded the possibility that the drug itself induced pro-inflammatory cytokine responses.

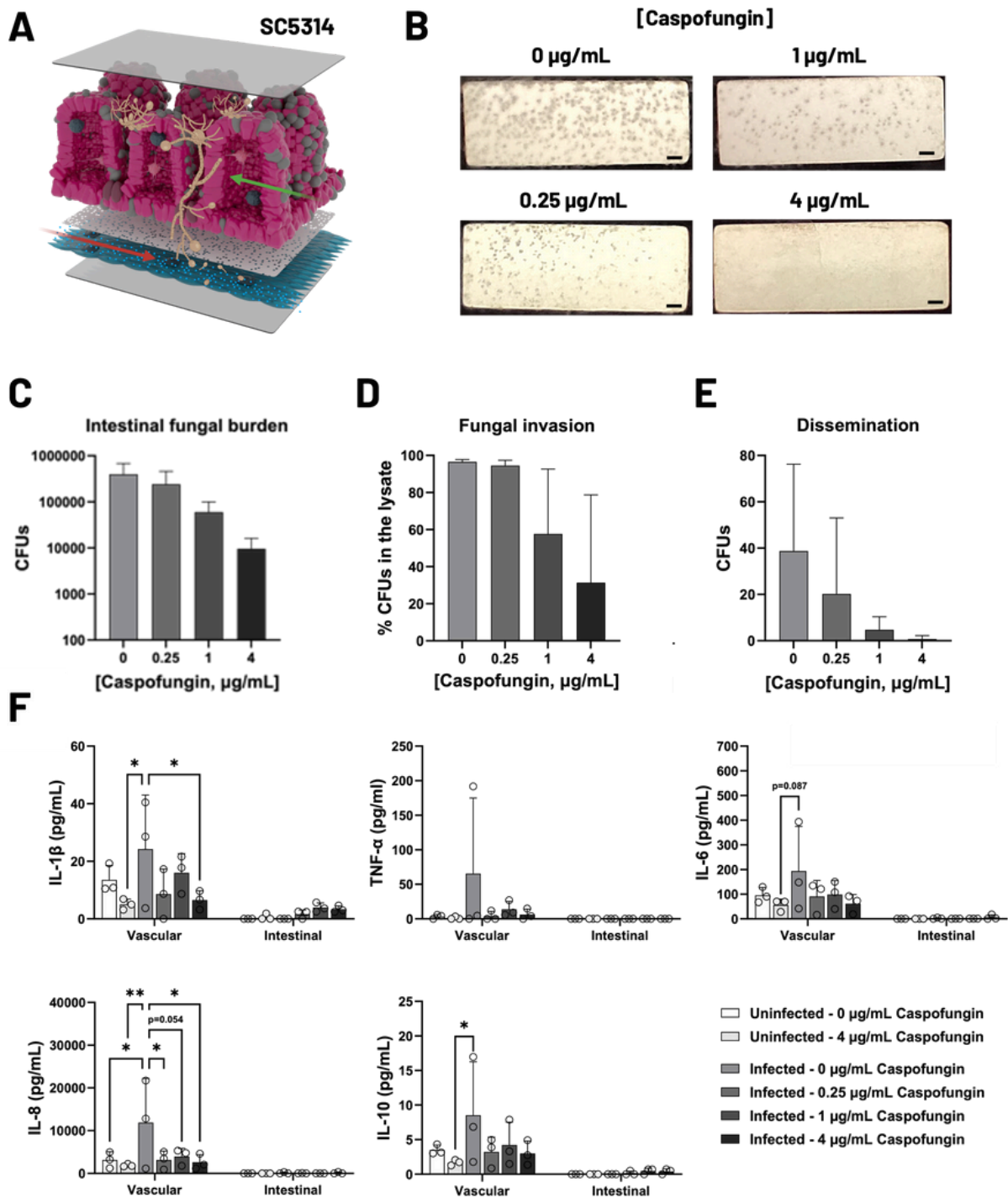


Figure 3: Effects of caspofungin perfusion in the candidiasis-on-chip model. A) Schematic model illustration showing *C. albicans* infection and vascular perfusion of antifungal caspofungin (blue dots). B) Representative images (from n = 4) of infected biochip membranes 24 hpi with *C. albicans* wild-type strain SC5314. Fungal microcolonies are macroscopically visible as fuzzy dots distributing homogeneously on the intestinal epithelial barrier. Increasing concentrations of caspofungin were applied in the vascular compartment of the biochip, altering the formation of microcolonies. Scale bars = 1 mm. C-E) Measurement of intestinal fungal burden from intestinal medium supernatants (C), fungal invasion in lysed intestinal and vascular cells (D), and dissemination in the perfused vascular medium supernatants (E) in infected models with caspofungin concentrations of 0, 0.25, 1, and 4 $\mu\text{g/mL}$. Bars illustrate mean \pm SD of 3 independent experiments (n = 3). F) Quantification of released vascular and intestinal cytokines (IL-1 β , TNF- α , IL-6, IL-8, IL-10) in uninfected or infected models treated with different concentrations of caspofungin for 24 h. Bars represent mean \pm SD of 3 independent experiments (n = 3) with three independent MDM donors. *p \leq 0.05, **p \leq 0.01 (Two-way ANOVA with Tukey's multiple comparison test).

4. Modeling antifungal drug resistance by testing the effectiveness of caspofungin on an echinocandin-resistant *C. albicans* strain

The model was further used to explore the behavior of a caspofungin-resistant clinical isolate 110.12 of *C. albicans* (Lackner et al., 2014) in response to caspofungin treatment within the chip model (Figure 4A). To address potential resistance, caspofungin concentrations were increased to 1, 4, and 6 $\mu\text{g/mL}$. Despite caspofungin administration, *C. albicans* 110.12 was able to form macroscopically visible microcolonies at all tested caspofungin concentrations 24 hpi (Figure 4B). No differences in microcolony amount were revealed between the different concentrations. While caspofungin was able to induce a concentration-dependent reduction in the intestinal fungal burden (Figure 4C), the efficacy was drastically diminished compared to the wild-type strain, even at the highest concentration. Tissue invasion remained high in contrast to the wild-type (Figure 4D). Although fungal translocation to the vascular compartment was reduced (Figure 4E), colony-forming units (CFUs) were consistently retrieved, indicating persistent invasive candidiasis. Infection with 110.12 led to elevated levels of IL-1 β , TNF- α , IL-6, IL-8, and IL-10 (Figure 4F). Unlike with the wild-type strain, caspofungin concentrations up to 4 $\mu\text{g/mL}$ had limited impact on reducing cytokine levels, except for TNF- α . Caspofungin significantly decreased TNF- α and IL-10 levels and induced decreasing trends for IL-8, IL-6, and IL-1 β . These findings highlight the challenges of treating infections caused by resistant *C. albicans* strains with reduced antifungal drug effectiveness.

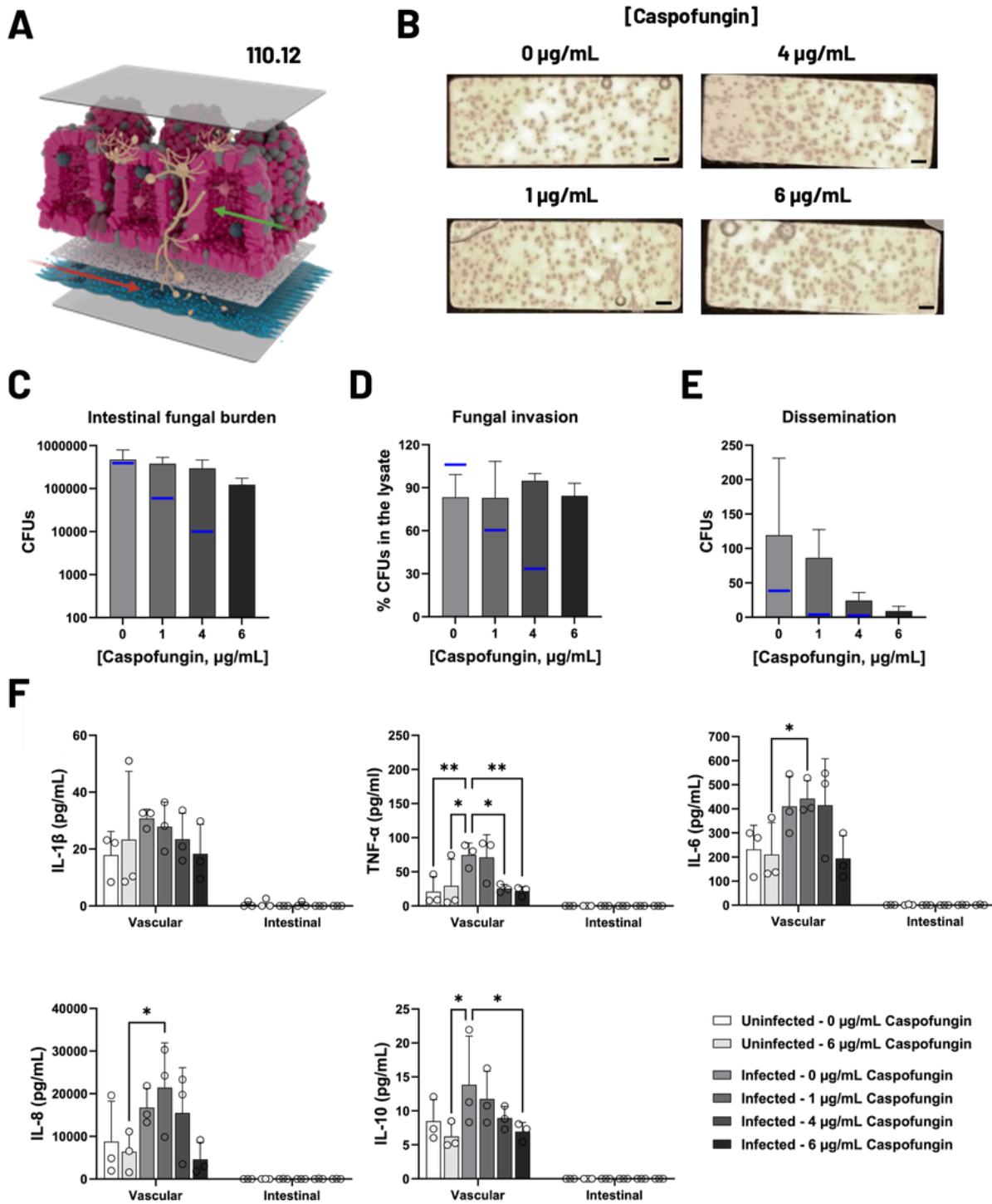


Figure 4: Effects of caspofungin on an echinocandin-resistant clinical isolate of *C. albicans*. A) Schematic model illustration demonstrating infection with an echinocandin-resistant *C. albicans* 110.12 and vascular perfusion of antifungal caspofungin (blue dots). B) Representative images (from $n = 3$) of infected biochip membranes 24 hpi with *C. albicans* strain 110.12. Scale bars = 1 mm. C-E) Measurement of intestinal fungal burden from intestinal medium supernatants (C), fungal invasion in lysed intestinal and vascular cells (D), and dissemination in the perfused vascular medium supernatants (E) in infected models with caspofungin concentrations of 0, 1, 4, and 6 $\mu\text{g/mL}$. Bars illustrate mean \pm SD of 3 independent experiments ($n = 3$). Blue lines indicate the mean from the wild-type *C. albicans* SC5314 strain. F) Quantification of released vascular and intestinal cytokines (IL-1 β , TNF- α , IL-6, IL-8, IL-10) in uninfected or infected models treated with different concentrations of caspofungin for 24 h. Bars represent mean \pm SD of 3 independent experiments ($n = 3$) with three independent MDM donors. * $p < 0.05$, ** $p < 0.01$ (Two-way ANOVA with Tukey's multiple comparison test).

5. In-depth image-based analysis of fungal objects

Morphometric analysis further revealed distinct morphological changes in response to caspofungin treatment (Figure 5). For the wild-type strain SC5314, caspofungin treatment led to a concentration-dependent reduction of microcolony number (Figure 5A), fungal object volume (Figure 5B), decrease of surface area-to-volume ratio (SA:V, Figure 5D), and an increase in microcolony compactness (Figure 5C). The decrease in surface area-to-volume ratio and the increase in denser microcolony structures suggest a reduced potential for interactions with the surrounding environment, which may reflect a survival mechanism under antifungal pressure.

These structural and morphological changes were not observed in the clinical isolate 100.12, which maintained a consistent number of microcolonies and similar morphometrics compared to infected models without caspofungin treatment.

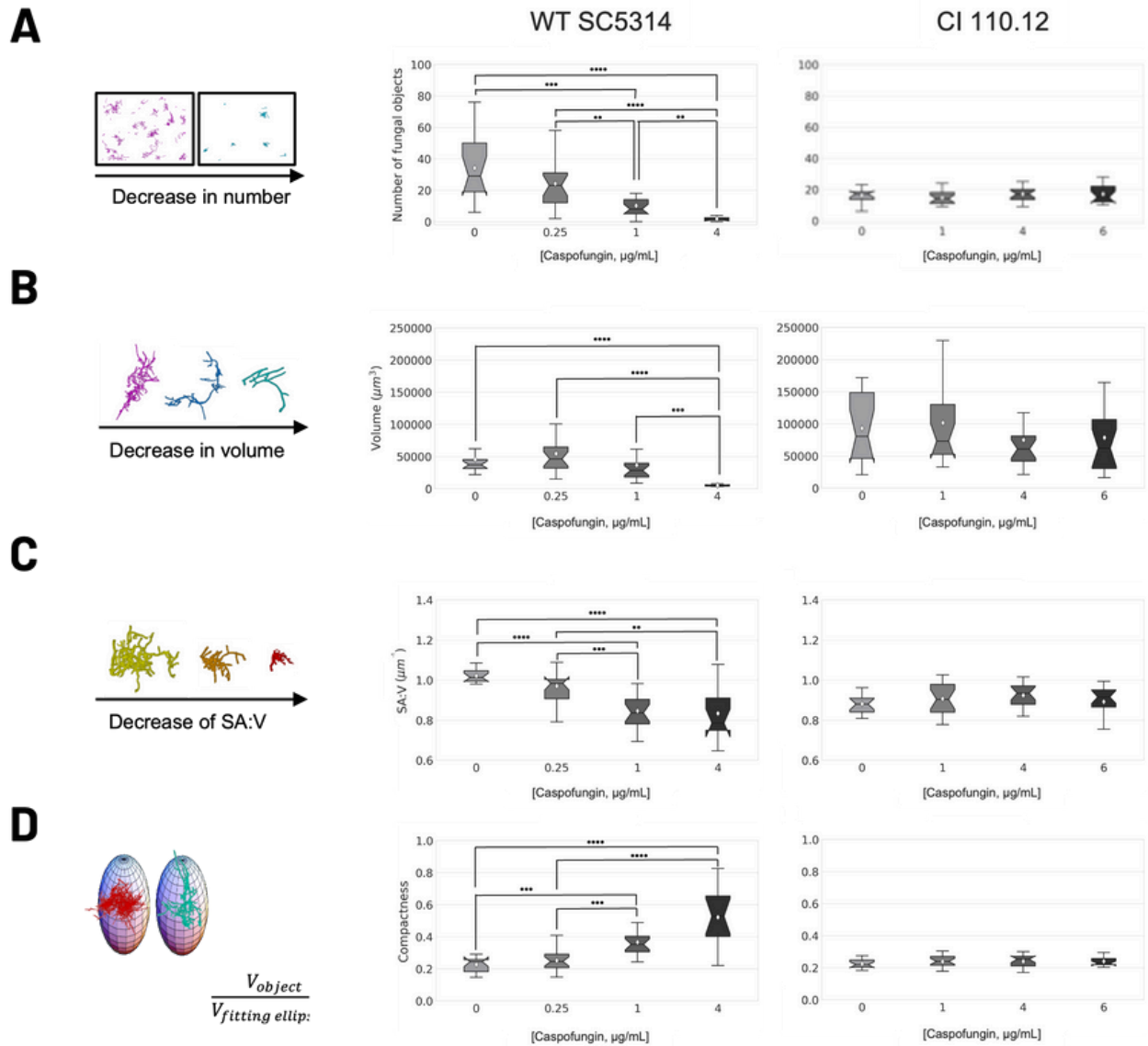


Figure 5: Morphometrics of fungal growth of *C. albicans* wild-type strain SC5314 and clinical isolate 110.12 with and without caspofungin treatment. Automated image analysis was used to quantify the number of fungal objects (A), and morphometric features per sample (averaged across fungal objects within the sample), i.e. the volume (B), the surface-area-to-volume (SA:V) ratio (C), and the compactness (D). **p < 0.01, ***p < 0.001, ****p < 0.0001 (Kruskal-Wallis test with Benjamini-Hochberg adjustment).

Conclusion

This study used an intestine-on-chip platform to evaluate *C. albicans* microcolony formation, invasion, and dissemination, simulating key processes of systemic candidiasis. It was demonstrated that the formation of microcolonies caused significant tissue damage in close proximity. Moreover, inflammation and barrier permeability were increased upon infection, leading to enhanced translocation of *C. albicans*. Vascular perfusion of caspofungin mimicked the intravenous administration route of the drug. Caspofungin reduced fungal microcolonies and induced substantial alterations in morphometrics such as size, surface-to-volume rate, and compactness, resulting in reduced pathogenicity. However, the resistant isolate showed limited sensitivity against caspofungin, with minimal effects of the drug on fungal burden and morphometrics, even at high concentrations. Caspofungin efficacy in this model required higher concentrations compared to a 2D *in vitro* system (data can be accessed in the original manuscript), implicating that compartmentalized 3D tissue structures and physiological drug administration routes can alter the effective concentration range of antifungal drugs.

Moreover, the 3D image analysis pipeline allowed for characterization of fungal morphology, quantification of tissue architecture, and co-localization of fungal objects and different tissue structures. This analysis suggested that *C. albicans* had a preferred niche in the areas of high-density tissue, equivalent to villus-like structures after attaching to the tissue (data can be accessed in the original manuscript). This behavior might be driven by more favorable growth conditions outside the tissue, suggesting that invasion primarily serves as an anchor to persist under peristaltic flow. The effects of more physiological relevant media (nutrient-poor, including microbiota, host-derived factors, and metabolites) in the intestinal side have yet to be explored.

Future improvements could include the integration of patient-derived cells, testing of combinatory antifungal drug treatments, and expanding to multi-organ systems to explore systemic dissemination and associated complications in other relevant organs.

In conclusion, this study demonstrates the potential of the intestine-on-chip model as a valuable tool for studying *C. albicans* pathogenesis and the efficacy of caspofungin. Due to its biological scalability, the model can be adapted for a variety of infectious diseases and can be useful for assessing alterations in host-microbiota interactions, effectiveness of antimicrobial drug treatment, and investigation of emerging drug resistances.

Key takeaways

- The intestine-on-chip candidiasis model recapitulates *C. albicans* infection processes such as microcolony formation, tissue invasion, vascular translocation and associated host damage
- Vascular perfused caspofungin reduces *C. albicans* pathogenicity and preserves tissue integrity only for the wild-type strain but not the echinocandin-resistant isolate
- By combining organ-on-chip technology with microbiological and advanced image-based analyses, it is possible to evaluate the effectiveness of antifungal drug treatments, emerging drug resistances, and personalized strategies in a scalable manner

References

- Allert, S., Förster, T. M., Svensson, C.-M., Richardson, J. P., Pawlik, T., Hebecker, B., Rudolphi, S., Juraschitz, M., Schaller, M., Blagojevic, M., Morschhäuser, J., Figge, M. T., Jacobsen, I. D., Naglik, J. R., Kasper, L., Mogavero, S., & Hube, B. (2018). *Candida albicans*-Induced Epithelial Damage Mediates Translocation through Intestinal Barriers. *mBio*, 9(3), e00915-18. <https://doi.org/10.1128/mBio.00915-18>
- Alonso-Roman, R., Last, A., Mirhakkak, M. H., Sprague, J. L., Möller, L., Großmann, P., Graf, K., Gratz, R., Mogavero, S., Vylkova, S., Panagiotou, G., Schäuble, S., Hube, B., & Gresnigt, M. S. (2022). *Lactobacillus rhamnosus* colonisation antagonizes *Candida albicans* by forcing metabolic adaptations that compromise pathogenicity. *Nature Communications*, 13(1), 3192. <https://doi.org/10.1038/s41467-022-30661-5>
- Balish, E., Warner, T. F., Nicholas, P. J., Paulling, E. E., Westwater, C., & Schofield, D. A. (2005). Susceptibility of Germfree Phagocyte Oxidase- and Nitric Oxide Synthase 2-Deficient Mice, Defective in the Production of Reactive Metabolites of Both Oxygen and Nitrogen, to Mucosal and Systemic Candidiasis of Endogenous Origin. *Infection and Immunity*, 73(3), 1313-1320. <https://doi.org/10.1128/IAI.73.3.1313-1320.2005>
- Fisher, M. C., Alastruey-Izquierdo, A., Berman, J., Bicanic, T., Bignell, E. M., Bowyer, P., Bromley, M., Brüggemann, R., Garber, G., Cornely, O. A., Gurr, Sarah. J., Harrison, T. S., Kuijper, E., Rhodes, J., Sheppard, D. C., Warris, A., White, P. L., Xu, J., Zwaan, B., & Verweij, P. E. (2022). Tackling the emerging threat of antifungal resistance to human health. *Nature Reviews Microbiology*, 20(9), 557-571. <https://doi.org/10.1038/s41579-022-00720-1>
- Gouba, N., & Drancourt, M. (2015). Digestive tract mycobiota: A source of infection. *Médecine et Maladies Infectieuses*, 45(1-2), 9-16. <https://doi.org/10.1016/j.medmal.2015.01.007>
- Graf, K., Last, A., Gratz, R., Allert, S., Linde, S., Westermann, M., Gröger, M., Mosig, A. S., Gresnigt, M. S., & Hube, B. (2019). Keeping *Candida* commensal: How lactobacilli antagonize pathogenicity of *Candida albicans* in an in vitro gut model. *Disease Models & Mechanisms*, 12(9), dmm039719. <https://doi.org/10.1242/dmm.039719>
- Kobayashi-Sakamoto, M., Tamai, R., Isogai, E., & Kiyoura, Y. (2018). Gastrointestinal colonisation and systemic spread of *Candida albicans* in mice treated with antibiotics and prednisolone. *Microbial Pathogenesis*, 117, 191-199. <https://doi.org/10.1016/j.micpath.2018.02.043>

Koh, A. Y., Köhler, J. R., Coggshall, K. T., Van Rooijen, N., & Pier, G. B. (2008). Mucosal Damage and Neutropenia Are Required for *Candida albicans* Dissemination. *PLoS Pathogens*, 4(2), e35. <https://doi.org/10.1371/journal.ppat.0040035>

Lackner, M., Tscherner, M., Schaller, M., Kuchler, K., Mair, C., Sartori, B., Istel, F., Arendrup, M. C., & Lass-Flörl, C. (2014). Positions and Numbers of FKS Mutations in *Candida albicans* Selectively Influence In Vitro and In Vivo Susceptibilities to Echinocandin Treatment. *Antimicrobial Agents and Chemotherapy*, 58(7), 3626–3635. <https://doi.org/10.1128/AAC.00123-14>

Maurer, M., Gresnigt, M. S., Last, A., Wollny, T., Berlinghof, F., Pospich, R., Cseresnyes, Z., Medyukhina, A., Graf, K., Gröger, M., Raasch, M., Siwczak, F., Nietzsche, S., Jacobsen, I. D., Figge, M. T., Hube, B., Huber, O., & Mosig, A. S. (2019). A three-dimensional immunocompetent intestine-on-chip model as in vitro platform for functional and microbial interaction studies. *Biomaterials*, 220, 119396. <https://doi.org/10.1016/j.biomaterials.2019.119396>

Mellado, E., Cuenca-Estrella, M., Regadera, J., González, M., Díaz-Guerra, T. M., & Rodríguez-Tudela, J. L. (2000). Sustained gastrointestinal colonization and systemic dissemination by *Candida albicans*, *Candida tropicalis* and *Candida parapsilosis* in adult mice. *Diagnostic Microbiology and Infectious Disease*, 38(1), 21–28. [https://doi.org/10.1016/S0732-8893\(00\)00165-6](https://doi.org/10.1016/S0732-8893(00)00165-6)

Miranda, L. N., Van Der Heijden, I. M., Costa, S. F., Sousa, A. P. I., Sienra, R. A., Gobara, S., Santos, C. R., Lobo, R. D., Pessoa, V. P., & Levin, A. S. (2009). *Candida* colonisation as a source for candidaemia. *Journal of Hospital Infection*, 72(1), 9–16. <https://doi.org/10.1016/j.jhin.2009.02.009>

Naglik, J. R., Fidel, P. L., & Odds, F. C. (2008). Animal models of mucosal *Candida* infection: Animal models of mucosal *Candida* infection. *FEMS Microbiology Letters*, 283(2), 129–139. <https://doi.org/10.1111/j.1574-6968.2008.01160.x>

Pfaller, M. A., Diekema, D. J., Rinaldi, M. G., Barnes, R., Hu, B., Veselov, A. V., Tiraboschi, N., Nagy, E., & Gibbs, D. L. (2005). Results from the ARTEMIS DISK Global Antifungal Surveillance Study: A 6.5-Year Analysis of Susceptibilities of *Candida* and Other Yeast Species to Fluconazole and Voriconazole by Standardized Disk Diffusion Testing. *Journal of Clinical Microbiology*, 43(12), 5848–5859. <https://doi.org/10.1128/JCM.43.12.5848-5859.2005>

Ruiz Mendoza, S., Liedke, S. C., Rodriguez De La Noval, C., Ferreira, M. D. S., Gomes, K. X., Honorato, L., Nimrichter, L., Peralta, J. M., & Guimarães, A. J. (2022). In vitro and in vivo efficacies of Dectin-1-Fc(IgG)(s) fusion proteins against invasive fungal infections. *Medical Mycology*, 60(8), myac050. <https://doi.org/10.1093/mmy/myac050>

Stone, J. A., Holland, S. D., Wickersham, P. J., Sterrett, A., Schwartz, M., Bonfiglio, C., Hesney, M., Winchell, G. A., Deutsch, P. J., Greenberg, H., Hunt, T. L., & Waldman, S. A. (2002). Single- and Multiple-Dose Pharmacokinetics of Caspofungin in Healthy Men. *Antimicrobial Agents and Chemotherapy*, 46(3), 739-745. <https://doi.org/10.1128/AAC.46.3.739-745.2002>

Wisplinghoff, H., Bischoff, T., Tallent, S. M., Seifert, H., Wenzel, R. P., & Edmond, M. B. (2004). Nosocomial Bloodstream Infections in US Hospitals: Analysis of 24,179 Cases from a Prospective Nationwide Surveillance Study. *Clinical Infectious Diseases*, 39(3), 309-317. <https://doi.org/10.1086/421946>

Zhai, B., Ola, M., Rolling, T., Tosini, N. L., Joshowitz, S., Littmann, E. R., Amoretti, L. A., Fontana, E., Wright, R. J., Miranda, E., Veelken, C. A., Morjaria, S. M., Peled, J. U., Van Den Brink, M. R. M., Babady, N. E., Butler, G., Taur, Y., & Hohl, T. M. (2020). High-resolution mycobiota analysis reveals dynamic intestinal translocation preceding invasive candidiasis. *Nature Medicine*, 26(1), 59-64. <https://doi.org/10.1038/s41591-019-0709-7>



Get in touch

Email
info@dynamic42.com

Web
dynamic42.com

Join us



Head Office
+49 (0) 3641 508101

Dynamic42 GmbH
Winzerlaer Straße 2
07745 Jena
Germany